Uranyl Sequestering Agents: Correlation of Properties and Efficacy with Structure for UO$_2^{2+}$ Complexes of Linear Tetradentate 1-Methyl-3-hydroxy-2(1H)-pyridinone Ligands[1]

Jide Xu and Kenneth N. Raymond*

Department of Chemistry and Chemical Sciences Division, Lawrence Berkeley National Laboratory, University of California, Berkeley, CA 94720

A rational design of uranyl sequestering agents based on 3-hydroxy-2(1H)-pyridinone ligands has resulted in the first effective agents for mammalian uranyl decorporation. In this study crystal structures of uranyl complexes with four of these agents are compared and correlated with the chemical and biological properties. These hydroxypyridinone ligands bind the uranyl ion in the equator of a pentagonal prism; a solvent molecule fills the fifth coordination site. The tetradentate ligands are composed of two hydroxypyridonate groups connected by a diamine linker via amide coupling. The dihedral angles between two pyridinone ring planes in these complexes differ as the length of linear backbone changes, giving these molecules a ruffled shape. The physical parameters (such as NMR chemical shifts) of the uranyl complexes with tetradentate Me-3,2-HOPO ligands correlate with the length of the diamine linker, as does the in vivo activity. The ligands are amides of 3-hydroxy-N-methyl-2-(1H)-4-carboxypyridone. For L^1 the amine is propane amine. For the tetradentate bis-amides the linker groups are (L^3) 1,3-diaminopropane, (L^4) 1,4-diaminobutane, (L^5) 1,5-diaminopentane. Crystal data: [UO$_2$(L^1)$_2$·DMF], space group, $C2/c$, cell constants: $a = 37.430(8)$ Å, $b = 7.0808(14)$ Å, $c = 26.781(5)$ Å, $\beta = 130.17(3)°$, $V = 5424(2)$ Å^3, $Z = 8$. [UO$_2$L^3·DMSO], $Pnma$, $a = 8.4113(1)$ Å, $b = 16.0140(3)$ Å, $c = 16.7339(3)$ Å, $V = 2254.03-(5)$ Å^3, $Z = 4$. [UO$_2$L^4·DMSO]·DMSO·H$_2$O·0.5C$_6$H$_{12}$, $P2_1/n$, $a = 26.7382(4)$ Å, $b = 7.4472(1)$ Å, $c = 31.4876-(2)$ Å, $V = 6209.05(13)$ Å^3, $Z = 8$. [UO$_2$L^5·DMSO]·DMSO, $Pnma$, $a = 7.3808(1)$ Å, $b = 14.7403(3)$ Å, $c = 23.1341(3)$ Å, $V = 2516.88(8)$ Å^3, $Z = 4$.

Introduction

A goal of the research in this laboratory has been the development of specific chelators for the actinides.[2−6] One important application of such agents is chelation therapy to remove accidentally incorporated actinides, thereby reducing health hazards caused by internal deposits of α-particle emitting radionuclides.[7] Several multidentate ligands prepared in this laboratory (containing catecholamide (CAM) or hydroxypyridinone (HOPO) metal binding units attached to suitable molecular linkers through amide linkages) are highly effective in animal models for decorporation of Pu(IV), Th(IV), and Am(III).[8−14]
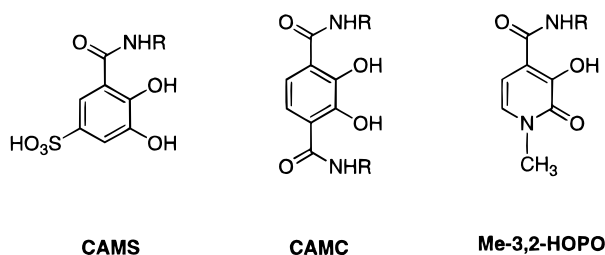
Uranium(VI) (UO$_2^{2+}$) causes kidney damage from chemical interactions,[15,16] and internally deposited high specific activity uranium isotopes can cause bone cancer.[17] Although sought for many years, no synthetic ligand has been able to reduce significantly the deposition of toxic amounts of uranyl ion in tissues, particularly kidney and bone.[18−21] Increased handling of uranium in the nuclear fuel cycle worldwide and the threat

---

* To whom correspondence should be addressed.

(1) This paper is number 39 in the series "Specific Sequestering Agents for the Actinides". The previous papers in this series (the most recent given first) are: Durbin, P. W.; Kullgren, B.; Xu, J.; Raymond, K. N.; Allen, P. G.; Bucher, J. J.; Edelstein, N. M.; Shuh, D. K. *Health Phys.* **1998**, *75*, 34−50; Volf, V.; Burgada, R.; Raymond, K. N.; Durbin; P. W. *Int. J. Radiat. Biol.* **1996**, *70*, 765−772; refs 30 and 11 in this paper; Volf, V.; Burgada, R.; Raymond, K. N.; Durbin, P. W. *Int. J. Radiat. Biol.* **1996**, *70*, 109−114; Stradling, G. N.; Gray, S. A.; Pearce, M. J.; Wilson, I.; Moody, J. C.; Hodgson, A.; Raymond, K. N. NRPB-M534 Report, January, 1995.

(2) Durbin, P. W.; Raymond K. N. *The Design, Synthesis and Evaluation of Sequestering Agents Specific for Plutonium(IV)*; Proceedings of The First Hanford Separation Science Workshop, July 23−25, 1991, Richland, WA; Publication PNL-SA-21775, 1993.

(3) Raymond, K. N. In *Environmental Inorganic Chemistry*: VCH Publishers: Deerfield Beach, FL, 1985; pp 331−347.

(4) Raymond, K. N.; Freeman, G. E.; Kappel, M. J. *Inorg. Chem. Acta* **1984**, *94*, 193−204.

(5) Franczyk, T. S.; Czerwinski; K. R.; Raymond, K. N. *J. Am. Chem. Soc.* **1992**, *114*, 8138−8146.

(6) Walton, P. H.; Raymond, K. N. *Inorg Chim. Acta* **1996**, *240*, 593.

(7) Raymond, K. N.; Smith, W. L. *Structure Bonding* **1981**, *43*, 159−186.

(8) Durbin, P. W.; Jeung, N.; Jones, E. S.; Weitl, F. L.; Raymond, K. N. *Radiat. Res.* **1984**, *99*, 85−105.

(9) White, D. L.; Durbin, P. W.; Jeung, N.; Raymond, K. N. *J. Med. Chem.* **1988**, *31*, 11−18.

(10) Xu, J.; Durbin, P. W.; Kullgren, B.; Raymond, K. N. *J. Med. Chem.* **1995**, *38*, 2606−2614.

(11) Durbin, P. W.; Kullgren, B.; Jeung, N.; Xu, J.; Rodgers, S. J.; Raymond, K. N. *Hum. Exp. Toxicol.* **1996**, *15*, 352−360.

(12) Stradling, G. N.; Gray, S. A.; Ellender, M.; Moody, J. C.; Hodgson, A.; Pearce, M.; Wilson, I.; Burgada, R.; Bailly, T. P.; Leroux; Y. G.; El Manouni, D.; Raymond, K. N.; Durbin, P. W. *Int. J. Radiat. Biol.* **1992**, *62*, 487−497.

(13) Volf, V.; Burgada, R.; Raymond, K. N.; Durbin, P. W. *J. Radiat. Biol.* **1993**, *63*, 785−793.

(14) Stradling, G. N.; Gray, S. A.; Pearce, M. J.; Wilson, I.; Moody, J. C.; Burgada, R.; Durbin, P. W.; Raymond, K. N. *Hum. Exp. Toxicol.* **1995**, *14*, 165−169.

(15) Hodge, H. C. In *Uranium, Plutonium, Transuranium Elements*; Springer-Verlag: Berlin, Germany, 1973; pp 5−68.

(16) Yuile, C. L. In: *Uranium, Plutonium, Transuranium Elements*; Springer-Verlag: Berlin, Germany, 1973; pp 165−196.

(17) Finkel, M. P. *Proc. Soc. Exp. Biol. Med.* **1953,** *83*, 494−498.

(18) Gindler, J. E. *Uranium, Plutonium, Transuranium Elements*; Springer-Verlag: Berlin, Germany, 1973; pp 69−164.

(19) Domingo, J. L.; Ortega, A.; Llobet, J. M.; Paternain, J. L.; Corbella, J. *Res. Commun. Pathol. Pharmacol.* **1989**, *64*, 161−164.

(20) Stradling, G. N.; Gray, S. A.; Moody, J. C.; Ellender, M. *Hum. Exp. Toxicol.* **1991**, *10*, 195−198.

(21) Archimbaud, M.; Henge-Napoli, M. H.; Lillienbaum, D.; Desloges, M.; Montagne, C. *Radiat. Prot. Dosim.* **1994**, *53*, 327−330.


Chart 1

CAMS   CAMC   Me-3,2-HOPO

Chart 2

PR-Me-3,2-HOPO, **HL**^{1}

2LI-Me-3,2-HOPO (n =1), **H$_2$L^2**
3LI-Me-3,2-HOPO (n =2), **H$_2$L^3**
4LI-Me-3,2-HOPO (n =3), **H$_2$L^4**
5LI-Me-3,2-HOPO (n =4), **H$_2$L^5**
6LI-Me-3,2-HOPO (n =5), **H$_2$L^6**

5LIO-Me-3,2-HOPO, **H$_2$L^7** ^{1R,2R}Cy-Me-3,2-HOPO, **H$_2$L^8**

of internal contamination of military personnel wounded with finely divided depleted uranium shrapnel has stimulated renewed interest in the development of uranium chelators suitable for human use.[22–26] The uranyl ion, a hard Lewis acid, has a high affinity for hard donor groups. Equatorial pentacoordination generally results from 5- and 6-membered chelate rings with bidentate ligands, as in [UO$_2$(acac)$_2$(H$_2$O)],[27] or with a small monodentate ligand, as in [UO$_2$(DMSO)$_5$]$^{2+}$.[28] The modest reduction of body uranium in animals by the injection of bidentate Tiron (4,5-dihydroxy-1,3-benzenedisulfonic acid, disodium salt),[19,20] and the favorable stability of the U(VI)-catechol complex (log K_{ML} = 15.9)[18] suggest that multidentate ligands containing the catecholate functionality or its structural analogues (such as hydroxypyridinones, HOPOs) as binding units might be effective for the in vivo chelation of U(VI). Based on the above observations, 10 multidentate ligands, with linear chain linkers containing sulfocatecholamide [CAM(S)], carboxycatecholamide [CAM(C)] or 3-hydroxy-*N*-methyl-2-(1*H*)-pyridone (Me-3,2-HOPO) as binding units (Chart 1) were designed to match the coordination environment of the uranyl ion. The ligands were injected into mice at a ligand/uranium molar ratio of about 90:1. Each of these ligands reduced whole body and kidney uranium, in most cases significantly, compared with U(VI)-injected control mice.[29,30] This demonstrated that these multidentate ligands are effective metal binding units for U(VI) in aqueous solution at physiological pH. The linear tetradentate ligands were, on average, more effective for reducing whole body and kidney uranium than the higher denticity ligands with branched chains. The animal test results also indicated that both the chain length and substituents on the linear aliphatic diamine linker of these tetradentate ligands play important roles in toxicity and efficacy for in vivo U(VI) chelation.[29,30]

To understand the relationship between the structure and the in vivo U(VI) chelation efficacy of the tetradentate ligands, we report here the design, syntheses, and characterizations of a series of tetradentate Me-3,2-HOPO ligands (Chart 2) and their uranyl complexes. The solid state structures of four uranyl complexes with bidentate and tetradentate Me-3,2-HOPO
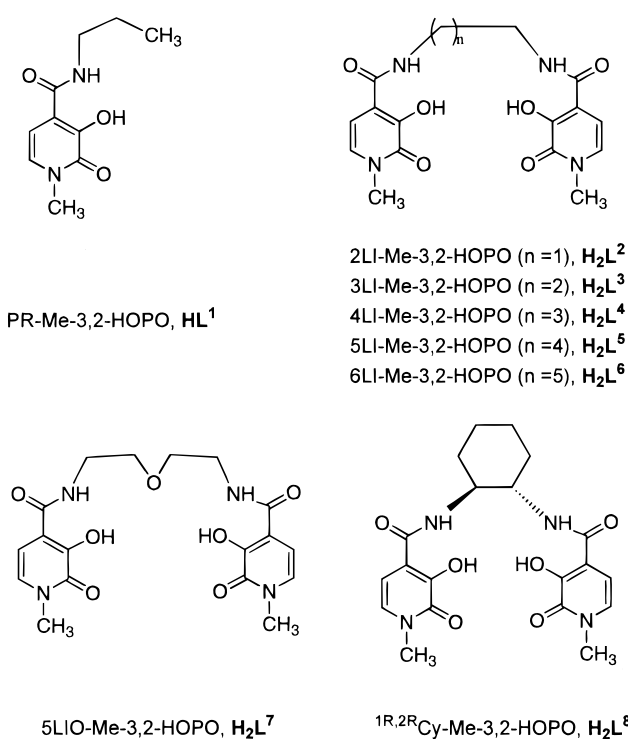
ligands have been determined by single crystal X-ray diffraction. These are the first fully characterized uranyl-hydroxypyridinone compounds.

Experimental Section

Synthesis of Tetradentate Me-3,2-HOPO Ligands. General. All chemicals were used as received from Aldrich unless otherwise noted. ^{1}H and ^{13}C NMR spectra were obtained on Bruker AMX-300 or DRX-500 spectrometers and are reported in ppm. Mass spectra and elemental (CHN) analyses were performed at the Elemental Analysis Facility, College of Chemistry, UC Berkeley. Unless specified, solvents were removed by rotary evaporation. 3-Benzyloxy-1-methyl-4-(2-thioxothiazolidin-1-yl)carbonyl-2(1*H*)-pyridone, bidentate PR-Me-3,2-HOPO (Chart 2) were synthesized by using the published general procedure.[10] To study the influence of ligand rigidity upon uranyl complexation, a series of tetradentate ligands with different linker lengths, 2LI-Me-3,2-HOPO, 3LI-Me-3,2-HOPO, 4LI-Me-3,2-HOPO, 5LI-Me-3,2-HOPO, 5LIO-Me-3,2-HOPO, 6LI-Me-3,2-HOPO and ^{1R,2R}Cy-Me-3,2-HOPO were synthesized (Chart 2).

2LI-Me-3,2-HOPOBn. The activated Me-3,2-HOPOBn-4-carboxylic acid, 3-benzyloxy-1-methyl-4-(2-thioxothiazolidin-1-yl)carbonyl-2(1*H*)-pyridone[10] (1.08 g, 3 mmol) was dissolved in dichloromethane, and a half equivalent of ethylenediamine (0.1 mL) was added with stirring. The solution was stirred until the yellow color of the activated thiazolide disappeared. This solution was extracted with a 1 M KOH solution and loaded onto a flash silica column. Elution with 4–7% methanol in dichloromethane yielded the benzyl-protected precursor (940 mg, 84.6%) as a white, microcrystalline solid. ^{1}H NMR (300 MHz, CDCl$_3$): δ 3.26 (t, J = 2.6, CH_2, 4H), 3.58 (s, CH_3, 6H), 5.34 (s, CH_2, 4H), 6.71 (d, J = 7.2 Hz, H_a, 2H), 7.14 (d, J = 7.2 Hz, H_b, 2H), 6.2–7.4 (m arom H, 10H), 8.02 (s, br, NH, 2H). ^{13}C NMR(500 MHz, CDCl$_3$): δ 37.5, 39.0, 74.4, 104.5, 128.4, 128.5, 128.7, 130.1, 131.9, 135.9, 146.1, 159.3, 163.5.

2LI-Me-3,2-HOPO (H$_2$L^2). In a round-bottom flask, 900 mg of 2LI-Me-3,2-HOPOBn was dissolved in a 1:1 mixture of glacial acetic acid and concentrated hydrochloric acid (30 mL), and the mixture was stirred at room temperature for 2 days. The reaction mixture was evaporated to dryness, and the residue was suspended in methanol (50 mL). The white precipitate was filtered and dried in a vacuum oven to yield a white powder (550 mg, 90%). Anal. Calcd (found) for C$_{16}$H$_{18}$N$_4$O$_6$

(22) Madic, C. *Radiat. Prot. Dosim.* **1989**, *26*, 15.
(23) *ATW–Int. Z. Kernenergie* **1996**, *41*, 478–479.
(24) Max, A.; Mason, T. *ATW–Int. Z. Kernenergie* **1996**, *41*, 79–84.
(25) Dietz, L. A. *Bull. Atomic Scientists* **1991**, *47*, 47.
(26) U.S. General Accounting Office. *Operation Desert Storm: Army not Adequately Prepared to Deal with Depleted Uranium Contamination*; GAO/NSIAD-93-90; U.S. General Accounting Office: Washington, DC, 1993.
(27) Frasson, E.; Bombieri, G.; Panattoni, C. *Coord. Chem. Rev.* **1966**, *1*, 145.
(28) Harrowfield, J. M.; Kepert, D. L.; Patrick, J. M.; White, A. H.; Lincoln, S. F. *J. Chem. Soc., Dalton Trans.* **1983**, 393–396.
(29) Durbin, P. W.; Kullgren, B.; Xu, J.; Raymond, K. N. *Radiat. Prot. Dosim.* **1994**, *53*, 305–309.
(30) Durbin, P. W.; Kullgren, B.; Xu, J.; Raymond, K. N. *Health Phys.* **1997**, *72*, 865–879.

(362.35): C, 53.03 (53.11); H, 5.00 (5.12); N, 15.46 (15.23). ^{1}H NMR (300 MHz, DMSO-d_6): δ 3.44 (s, NCH_3, NCH_2, 10H), 6.48 (d, J = 7.2 Hz, H_a, 2H), 7.18 (d, J = 7.0 Hz, H_b, 2H), 8.57 (s,br, NH, 2H), 11.47 (br, OH, 2H). ^{13}C NMR (500 MHz, DMSO-d_6): δ 36.82, 38.66, 102.62, 117.17, 127.72, 147.54, 158.03, 165.75. MS (+FAB, NBA): 363.2 (MH$^+$).

3LI-Me-3,2-HOPOBn. The benzyl-protected ligand was synthesized by a procedure similar to that of 2LI-Me-3,2-HOPOBn, except 1,3-diaminopropane was used instead of ethylenediamine. Separation and purification were performed as 2LI-Me-3,2-HOPOBn. It was obtained as a pale yellow oil, yield 82%. ^{1}H NMR (300 MHz, CDCl$_3$): δ 1.316 (qin, 2H, J = 6.7 Hz, NCH_2CH_2), 3.093 (q, 4H, J = 6.4 Hz, NHCH_2), 3.606 (s, 6H, NCH_3), 5.405 (s, 4H, benzyl CH_2), 6.751 (d, 2H, J = 7.2 Hz, HOPO ring H), 7.111 (d, 2H, J = 7.2 Hz, HOPO ring H), 7.27−7.44 (m, 10H, benzyl arom H), 7.957 (t, 3H, J = 5.6 Hz, amide H). ^{13}C NMR (500 MHz, CDCl$_3$): δ 28.4, 36.4, 38.9, 74.1, 104.7, 128.4, 128.5, 128.7, 130.5, 131.8, 136.2, 146.0, 159.4, 163.4. MS (+FAB, NBA): 557.3 (MH$^+$).

3LI-Me-3,2-HOPO (H$_2$L^3). The above protected ligand was deprotected following the procedure used for 2LI-Me-3,2-HOPOBn. It was obtained as a white solid, yield 89%. Anal. Calcd (found) for C$_{17}$H$_{20}$N$_4$O$_6$ (376.375): C, 54.25 (54.17); H, 5.35 (5.49); N, 14.88 (14.59). ^{1}H NMR (300 MHz, DMSO-d_6): δ 1.757 (t, 2H, −NCH_2CH_2), 3.327 (q, 4H, NH-CH_2), 3.469 (s, 6H, NCH_3), 6.503 (d, 2H, J = 7.2 Hz, HOPO ring H), 7.193 (d, 2H, J = 7.2 Hz, HOPO ring H), 8.483 (s,br, 2H, amide H), 11.7 (s, br, 2H, phenol H). ^{13}C NMR (500 MHz, DMSO-d_6): 28.8, 36.8, 39.0, 102.4, 116.9, 127.6, 148.1, 158.0, 165.9. MS (+FAB, NBA): 377.2 (MH$^+$).

4LI-Me-3,2-HOPOBn. The benzyl protected ligand was synthesized by a procedure similar to that of 2LI-Me-3,2-HOPOBn, except 1,4-diaminopropane was used instead of ethylenediamine. It was obtained as a white crystalline solid, yield 87%. ^{1}H NMR (300 MHz, CDCl$_3$): δ 1.140 (s,br, 4H, −NCH_2CH_2), 3.110 (d,br, 4H, J = 5.6 Hz, NHC$_2$), 3.606 (s, 6H, NCH_3), 5.365 (s, 4H, benzyl-CH_2), 6.801 (d, 2H, J = 7.2 Hz, HOPO ring H), 7.129 (d, 2H, J = 7.2 Hz, HOPO ring H), 7.27−7.44 (m, 10H, benzyl arom H), 7.849 (t, 2H, J = 5.2 Hz, amide H). ^{13}C NMR (500 MHz, CDCl$_3$): 26.6, 37.2, 39.0, 74.5, 104.5, 128.3, 128.4, 128.5, 130.0, 131.8, 135.7, 146.0, 159.1, 162.5. Ms (+FAB, NBA): 571.2 (MH$^+$).

4LI-Me-3,2-HOPO (H$_2$L^4). The above protected ligand was deprotected following the procedure used for 2LI-Me-3,2-HOPOBn. It was obtained as a white solid, yield 89%. Anal. Calcd (found) for C$_{18}$H$_{22}$N$_4$O$_6$·0.5H$_2$O (399.41): C, 54.13 (54.17); N, 14.02 (13.89). ^{1}H NMR (300 MHz, DMSO-d_6): δ 1.541 (s,br, 2H, −NCH_2CH_2), 3.308 (s,br, 4H, N-CH_2), 3.463 (s, 6H, N-CH_3), 6.515 (d, 2H, J = 7.3 Hz, HOPO ring H), 7.187 (d, 2H, J = 7.3 Hz, HOPO ring H), 8.483 (t,br, 2H, J = 5.3 Hz, amide H). ^{13}C NMR (500 MHz, DMSO-d_6): 26.4, 36.8, 38.7, 102.3, 116.9, 127.7, 148.0, 158.0, 165.7. MS (+FAB, NBA): 391.3 (MH$^+$).

5LI-Me-3,2-HOPOBn. The benzyl protected ligand was synthesized by a procedure similar to that of 2LI-Me-3,2-HOPOBn, except 1,5-diaminopropane was used instead of ethylenediamine. It was obtained as a pale yellow oil, yield 73%. ^{1}H NMR (300 MHz, CDCl$_3$): δ 1.064 (m,br, 2H, NCH$_2$CH$_2$CH_2), 1.207 (qin,br, 4H, J = 7.0 Hz, NCH$_2$CH_2), 3.134 (q, 4H, J = 5.5 Hz, NHCH_2), 3.605 (s, 6H, NCH_3), 5.367 (s, 4H, benzyl-CH_2), 6.803 (d, 2H, J = 7.2 Hz, HOPO ring H), 7.126 (d, 2H, J = 7.2 Hz, HOPO ring H), 7.28−7.45 (m, 10H, benzyl arom H), 7.872 (t, 2H, J = 4.6 Hz, amide H). ^{13}C NMR (500 MHz, CDCl$_3$): 23.5, 27.3, 36.9, 39.7, 74.5, 102.5, 128.4, 128.5, 128.6, 130.1, 131.9, 135.9, 146.1, 158.2, 163.7. MS (+FAB, NBA): 585.1 (MH$^+$).

5LI-Me-3,2-HOPO (H$_2$L^5). The above protected ligand was deprotected following the procedure used for 2LI-Me-3,2-HOPOBn. It was obtained as a white solid, yield 79%. Anal. Calcd (found) for C$_{19}$H$_{24}$N$_4$O$_6$·0.6H$_2$O (415.24): C, 54.96 (54.89); N, 13.45 (13.27). ^{1}H NMR (300 MHz, DMSO-d_6): δ 1.32 (m, 2H, NCH$_2$-CH$_2$CH_2), 1.527 (qin, 4H, J = 7.1 Hz, NCH$_2$CH_2), 3.276 (q, 4H, J = 6.5 Hz, NCH_2), 3.464 (s, 6H, NCH_3), 6.509 (d, 2H, J = 7.3 Hz, HOPO ring H), 7.183 (d, 2H, J = 7.3 Hz, HOPO ring H), 8.459 (t, br, 2H, J = 5.5 Hz, amide H). ^{13}C NMR (500 MHz, DMSO-d_6): 23.8, 28.5, 36.8, 39.0, 102.4, 117.0, 127.7, 148.0, 158.0, 165.7. MS (+FAB, NBA): 405 (MH$^+$).

6LI-Me-3,2-HOPOBn. This compound was prepared by a procedure similar to that of 2LI-Me-3,2-HOPOBn, except 1,6-hexanediamine was used instead of ethylenediamine. It was obtained as a pale yellow oil, yield 89%. ^{1}H NMR (300 MHz, CDCl$_3$): δ 1.09 (m, br, 2H, NCH$_2$-CH$_2$CH_2), 1.212 (t, br, 4H, J = 6.4 Hz, NCH$_2$CH_2), 3.176 (q, 4H, J = 6.4 Hz, NCH$_2$CH_2), 3.604 (s, 6H, NCH_3), 5.357 (s, 4H, benzyl CH_2), 6.813 (d, 2H, J = 7.2 Hz, HOPO ring H), 7.123 (d, 2H, J = 7.2 Hz, HOPO ring H), 7.27−7.45 (m, 10H, benzyl arom H), 7.897 (t, 2H, J = 5.0, amide H). ^{13}C NMR (500 MHz, CDCl$_3$): 26.2, 28.5, 37.3, 39.3, 74.5, 128.4, 128.5, 128.6, 130.2, 131.9, 135.9, 146.1, 159.1, 162.7. MS (+FAB, NBA): 599.4 (MH$^+$).

6LI-Me-3,2-HOPO (H$_2$L^6). The above protected ligand was deprotected following the procedure used for 2LI-Me-3,2-HOPOBn. It was obtained as a white solid, yield 83%. Anal. Calcd (found) for C$_{20}$H$_{26}$N$_4$O$_6$·0.25H$_2$O (422.96): C, 56.79 (57.03); H, 6.31 (6.41)); N, 13.24 (12.95). ^{1}H NMR (300 MHz, DMSO-d_6): δ 1.32 (s,br, 4H, NCH$_2$-CH$_2$CH_2), 1.501 (t, br, 4H, J = 6.4, NCH$_2$CH_2), 3.258 (q, 4H, J = 6.5, NCH_2), 3.452 (s, 6H, NCH_3), 6.502 (d, 2H, J = 7.2 Hz, HOPO ring H), 7.183 (d, 2H, J = 7.3 Hz, HOPO ring H), 8.455 (t, br, 2H, J = 5.4 Hz, amide H), 11.8 (s, br, phenol H). ^{13}C NMR (500 MHz, DMSO-d_6): 26.0, 28.8, 36.8, 39.0, 102.4, 117.0, 127.7, 148.0, 158.0, 165.6. MS (+FAB, NBA): 419.2 (MH$^+$).

5LIO-Me-3,2-HOPOBn. The benzyl protected ligand was synthesized by a procedure similar to that of 2LI-Me-3,2-HOPOBn, except 2-aminoethyl ether was used instead of ethylenediamine. It was obtained as a white crystalline solid, yield 79%. ^{1}H NMR (300 MHz, CDCl$_3$): δ 3.245 (t, 4H, J = 4.8 Hz, OCH_2), 3.309 (t, 4H, J = 4.8 Hz, NHCH_2), 3.593 (s, 6H, NCH_3), 5.271(s, 4H, benzyl-CH_2), 6.739 (d, 2H, J = 7.2 Hz, HOPO ring H), 7.125 (d, 2H, J = 7.2 Hz, HOPO ring H), 7.28−7.45 (m, 10H, benzyl arom H), 8.052 (t, 2H, J = 4.3 Hz, amide H). ^{13}C NMR (500 MHz, CDCl$_3$): 37.2, 39.1, 68.3, 74.5, 102.4, 116.9, 127.6, 148.1, 158.0, 1651. MS (+FAB, NBA): 587.3 (MH$^+$).

5LIO-Me-3,2-HOPO (H$_2$L^7). The above protected ligand was deprotected following the procedure used for 2LI-Me-3,2-HOPOBn. It was obtained as a white solid, yield 79%. Anal. Calcd (found) for C$_{18}$H$_{22}$N$_4$O$_7$ (406.40): C, 53.19 (53.38); H, 5.48 (5.59); N, 13.72 (13.62). ^{1}H NMR (300 MHz, DMSO-d_6): δ 3.327 (t, br, 4H, OCH$_2$CH_2), 3.404(s, 6H, NCH_3), 3.488(q, J = 5.4, NCH_2), 6.452 (d, 2H, J = 7.3 Hz, HOPO ring H), 7.107 (d, 2H, J = 7.3 Hz, HOPO ring H), 8.483 (t, br, 2H, J = 5.5 Hz, amide H). ^{13}C NMR (500 MHz, DMSO-d_6): 36.8, 38.9, 68.5, 102.7, 117.1, 127.7, 147.3, 158.1, 165.2. MS (+FAB, NBA): 407 (MH$^+$).

^{1R,2R}Cy-Me-3,2-HOPOBn. The benzyl-protected ligand was synthesized by coupling the activated Me-3,2-HOPO acid with enantiomerically pure 1R,2R-cis-diaminocyclohexane. The protected ligand was obtained as a pale yellow oil, yield 83%. ^{1}H NMR(300 MHz, CDCl$_3$): δ 0.76 (m, HCH, 2H), 1.15 (m, HCH, 2H), 1.57 (m, HCH, 2H), 1.77 (s, HCH, 1H), 1.82 (s, HCH, 1H), 3.55 (s, CH_3, 6H), 3.67 (m, HCH, 2H), 5.41 (s, benzyl CH_2, 2H), 6.66 (d, J = 7.2 Hz, H_a, 2H), 7.01 (d, J = 7.2 Hz, H_b, 2H), 7.2−7.5 (m, arom H, 10 H), 7.93 (d, NH, 2H). ^{13}C NMR(500 MHz, CDCl$_3$): δ 23.98, 31.20, 37.11, 52.62, 73.86, 104.27, 128.10, 128.19, 128.62, 129.96, 131.53, 136.03, 145.78, 159.03, 162.78.

^{1R,2R}Cy-Me-3,2-HOPO (H$_2$L^8). The benzyl-protected ligand was deprotected following the procedure used for 2LI-Me-3,2-HOPO. The deprotected ligand was obtained as a white solid, yield 89%. Anal. Calcd (found) for C$_{20}$H$_{24}$N$_4$O$_6$ (418.44): C, 57.68 (57.51); H, 5.81 (5.74); N, 13.45 (13.51). ^{1}H NMR(300 MHz, DMSO-d_6): δ 1.30 (m, HCH, 2H), 1.41 (m, HCH, 2H), 1.91(m, HCH, 2H), 1.69 (m, HCH, 2H) 3.91 (m, HCH, 2H), 6.42 (d, J = 7.2 Hz, H_a, 2H), 7.12(d, J = 7.2 Hz, H_b, 2H), 8.36 (d, J = 7.5 Hz, NH, 2H), 11.75 (s,br, OH, 2H). ^{13}C NMR(500 MHz, DMSO-d_6): δ 24.31, 31.52, 36.73, 52.31, 102.24, 116.60, 127.53, 148.08, 157.89, 165.59.

Synthesis of Uranyl Complexes. General. A solution of UO$_2$(ClO$_4$)$_2$·6H$_2$O (57.7 mg, 0.1 mmol) in CH$_3$OH was added to a methanol solution of a bidentate ligand (0.22 mmol) or a tetradentate ligand (0.11 mmol) with stirring. The colorless ligand solution immediately turned orange and showed a strong acidic reaction to pH paper, indicating the formation of a uranyl complex. Following the addition of 1 or 2 drops of pyridine the transparent reaction mixture became turbid. The solution was then heated at reflux overnight, under nitrogen. The uranyl

Table 1. X-ray Crystallographic Data for the Uranyl Bidentate and Tetradentate Me-3,2-HOPO Complexes Described

formula (Figure 1)	$[UO_2(L^1)_2 \cdot DMF]$	$[UO_2L^3 \cdot DMSO]$	$[UO_2L^4 \cdot DMSO] \cdot DMSO \cdot H_2O \cdot 0.5C_6H_{12}$	$[UO_2L^5 \cdot DMSO)] \cdot DMSO$
fw	761.58	722.52	878.80	768.85
cryst size, mm	$0.1 \times 0.1 \times 0.03$	$0.22 \times 0.18 \times 0.12$	$0.24 \times 0.16 \times 0.10$	$0.22 \times 0.12 \times 0.10$
cryst system	monoclinic	orthorhombic	monoclinic	orthorhombic
space group	*C2/c*	*Pnma*	*P2(1)/n*	*Pnma*
T, °C	$-90(2)$	$-126(2)$	$-120(2)$	$-140(2)$
a, Å	37.430(8)	8.4113(1)	26.7382(4)	7.3808(1)
b, Å	7.0808(14)	16.0140(3)	7.4472(1)	14.7403(3)
c, Å	26.781(5)	16.7339(1)	31.4876(2)	23.1341(5)
α, deg	90	90	90	90
β, deg	130.17(3)	90	97.993(1)	90
γ, deg	90	90	90	90
V, Å^3	5424(2)	2254.03(5)	6209.05(13)	2516.88(8)
Z	8	4	8	4
ρ_{calcd}, g·cm^{-3}	1.865	2.129	1.576	2.028
abs coeff, mm^{-1}	6.044	7.353	5.340	6.595
2θ range, deg	$2.84 \leq 2\theta \leq 46.48$	$3.52 \leq 2\theta \leq 46.46$	$2.16 \leq 2\theta \leq 46.52$	$3.28 \leq 2\theta \leq 46.48$
no. of indep reflcns	3855	1683	8864	1891
no. of parameters	343	164	793	182
R^a $[I > 2\sigma(I)]$	0.0371	0.0193	0.0373	0.0235
wR2^b $[I > 2\sigma(I)]$	0.0845	0.0494	0.0938	0.0586

^{a} $R = \sum ||F_o| - |F_c||/\sum |F_o|$. ^{b} wR2 $= \{\sum [w(F_o^2 - F_c^2)^2]/\sum [w(F_o^2)^2]\}^{1/2}$.

complexes deposited as orange precipitates, which were collected by filtration, washed with methanol, and dried in a vacuum oven.

Uranyl-PR-3,2-HOPO Complex (UO₂(L)¹₂·H₂O). Yield 77%. Anal. Calcd (found) for $UO_2C_{20}H_{26}N_4O_6 \cdot H_2O$ (706.50): C, 34.00 (34.04); H, 3.99 (4.01); N, 7.93 (7.81). ^1H NMR (300 MHz, DMSO-d_6): δ 1.07 (t, $J = 7.3$ Hz, CH_3, 6H), 1.73 (qint, $J = 7.2$ Hz, CH_2, 4H), 3.50 (q, $J = 6.4$ Hz, CH_2, 4H), 3.98 (s, br, CH_3, 6H), 7.12 (d, $J = 7.0$ Hz, H_a, 2H), 7.25 (d, $J = 7.0$, H_b, 2H), 9.96 (s, NH, 2H). (+FAB, NBA) = 689.2 (MH⁺).

Uranyl-2LI-Me-3,2-HOPO complex (UO₂L²·H₂O). Yield 92%. Anal. Calcd (found) for $UO_2C_{16}H_{16}N_4O_6 \cdot H_2O$ (648.37): C, 29.63 (29.84); H, 2.80 (3.01); N, 8.64 (8.47). ^1H NMR (300 MHz, DMSO-d_6): δ 3.70 (s, CH_2, 4H), 3.94 (s, CH_3, 6H), 7.03 (d, $J = 7.0$, H_a, 2H), 7.21 (s, $J = 7.0$, H_b, 2H), 10.99 (s, br, NH, 2H). MS (+FAB, NBA) = 631.1 (MH⁺).

Uranyl-3LI-Me-3,2-HOPO Complex (UO₂L³·H₂O). Yield 87%. Anal. Calcd (found) for $UO_2C_{17}H_{18}N_4O_6 \cdot H_2O$ (662.40): C, 30.82 (30.64); H, 3.04 (3.31); N, 8.46 (8.27). ^1H NMR (300 MHz, DMSO-d_6): δ 2.06 (t, CH_2, 2H), 3.69 (q, $J = 4.8$ Hz, CH_2, 4H), 3.95 (s, CH_3, 6H,), 7.10 (d, $J = 6.9$ Hz, H_a, 2H), 7.23 (s, $J = 7.2$ Hz, H_b, 2H), 10.16 (t, $J = 5.0$, NH, 2H). MS (+FAB, NBA) = 645.1 (MH⁺).

Uranyl-4LI-Me-3,2-HOPO Complex (UO₂L⁴·H₂O). Yield 84%. Anal. Calcd for $UO_2C_{18}H_{20}N_4O_6 \cdot H_2O$ (676.43): C, 31.96 (31.71); H, 3.28 (3.56); N, 8.28 (7.95). ^1H NMR (300 MHz, DMSO-d_6): δ 1.93(s, CH_2, 4H), 3.49(s, CH_2, 4H), 3.98 (s, CH_3, 6H), 7.11 (d, $J = 7.0$ Hz, H_a, 2H), 7.27 (s, $J = 7.0$ Hz, H_b, 2H), 9.26 (s,br, NH, 2H). MS (+FAB, NBA): 660.2 (MH⁺).

Uranyl-5LI-Me-3,2-HOPO Complex (UO₂L⁵·H₂O). Yield 81%. Anal. Calcd for $UO_2C_{19}H_{22}N_4O_6 \cdot H_2O$ (690.46): C, 33.05 (32.91); H, 3.50 (3.76); N, 8.11 (7.87). ^1H NMR (300 MHz, DMSO-d_6): δ 1.80 (s, CH_2, 4H), 3.60 (s, CH_2, 4H), 3.98 (s, CH_3, 6H), 7.14 (d, $J = 7.0$ Hz, H_a, 2H), 7.28 (s, $J = 7.0$ Hz, H_b, 2H), 9.45 (s,br, NH, 2H). MS (+FAB, NBA): 675.2 (MH⁺).

Uranyl-6LI-Me-3,2-HOPO Complex (UO₂L⁶·H₂O). Yield 88%. Anal. Calcd for $UO_2C_{20}H_{26}N_4O_6 \cdot 2H_2O$ (724.52): C, 33.15 (32.94); H, 4.17 (4.37); N, 7.73 (7.81). ^1H NMR (300 MHz, DMSO-d_6): δ 1.55 (br, CH_2, 2H), 1.61 (br, CH_2, 2H), 1.72 (br, CH_2, 4H), 3.48 (br, CH_2, 4H), 3.95 (br, CH_3, 6H), 7.11 (br, H_a, 2H), 7.27 (br, H_b, 2H), 9.51 (br, NH, 2H). MS (+FAB, NBA): 689.2 (MH⁺).

Uranyl-5LIO-Me-3,2-HOPO Complex (UO₂L⁷·H₂O). Yield 79%. Anal. Calcd for $UO_2C_{18}H_{20}N_4O_7 \cdot H_2O$ (692.43): C, 31.22 (30.94); H, 3.20 (3.37); N, 8.09 (7.81). ^1H NMR (300 MHz, DMSO-d_6): δ 3.77 (s, br, CH_2, 8H), 3.98 (s, CH_3, 6H), 7.14 (d, $J = 6.9$ Hz, H_a, 2H), 7.27 (s, $J = 7.2$ Hz, H_b, 2H), 9.76 (s,br, NH, 2H). MS (+FAB, NBA): 675.2 (MH⁺).

Uranyl-^{1R,2R}Cy-Me-3,2-HOPO Complex (UO₂L⁸·H₂O). Yield 79%. Anal. Calcd (found) for $UO_2C_{20}H_{22}N_4O_6 \cdot H_2O$ (702.44): C, 34.20

(34.11); H, 3.44 (3.53); N, 7.97 (7.79). ^1H NMR (300 MHz, DMSO-d_6): δ 1.55 (s, br, CH_2, 2H), 1.74 (s, br, CH_2, 2H), 1.91 (s, br, CH_2, 2H), 3.35 (s, br, CH_3, 6H), 4.00 (s, br, 6H), 4.41 (s, br, 2H), 6.93 (s, br, H_a, 2H), 7.11 (s, br, H_b, 2H), 9.96 (s, br, NH, 2H).

X-ray Crystallography. The uranyl complexes are sparingly soluble in water. X-ray-quality crystals of $[UO_2 (L^1)_2 \cdot DMF]$, $[UO_2 L^3 \cdot DMSO]$, $[UO_2 L^4 \cdot DMSO] \cdot DMSO \cdot H_2O \cdot 0.5C_6H_{12}$, and $[UO_2(L^5) \cdot DMSO] \cdot DMSO$ were obtained by diffusion of ether or cyclohexane into a DMF or DMSO solution of the corresponding complexes. Crystals were mounted in Paratone N oil on the ends of quartz capillaries and frozen into place under a low-temperature nitrogen cold stream. Data were collected on a Siemens SMART/CCD X-ray diffractometer[31] with Mo Kα radiation ($\lambda = 0.710$ 72 Å). The intensity data were extracted from the frames using the program SAINT.[32] Data analysis was performed using the Siemens XPREP program;[33] no decay correction was needed. A semiempirical absorption correction was applied to the data. The structures were solved by direct methods (SHELXTL)[34] and refined on F^2 using full-matrix least-squares. All non-hydrogen atoms were refined anisotropically. Hydrogen atoms were assigned to idealized positions and the isotropic thermal parameters set to 1.5 (methyl hydrogens) or 1.2 (all other hydrogens) times the thermal parameters of the adjacent carbon atoms. Crystallographic information is summarized in Table 1.

Results and Discussion

Design of Tetradentate Me-3,2-HOPO Uranium(VI) Sequestering Agents. The simple bidentate ligand PR-Me-3,2-HOPO[10] (HL¹ in Chart 1) was chosen as a model for the design of bis-bidentate Me-3,2-HOPO sequestering agents for UO_2^{2+}, since it presents minimum constraints on the geometry of the complex. Although crystals were not obtained from water, the other solvent molecules can be regarded as replacing it; X-ray structural analysis of $[UO_2(L^1)_2 \cdot DMF]$ indicated that the uranyl is equatorially coordinated in a slightly distorted pentagonal bipyramidal geometry. Four of the equatorially ligating atoms are the HOPO oxygens of two independent ligands and the remaining coordination site is occupied by the solvent (DMF) oxygen atom O7, as shown in Figure 1a.

(31) *SMART Area Detector Software Package*; Siemens Industrial Automation, Inc.: Madison, WI, 1995.
(32) *SAINT: SAX Area-Detector Integration Program*, V.4.024; Siemens Industrial Automation, Inc.: Madison, WI, 1995.
(33) *XPREP (V. 5.03), Part of SHELXTL Crystal Structure Determination Package*; Siemens Industrial Automation, Inc.: Madison, WI, 1995.
(34) *SHELXTL (V. 5.03), SHELXTL Crystal Structure Determination Package*; Siemens Industrial Automation, Inc.: Madison, WI, 1995.
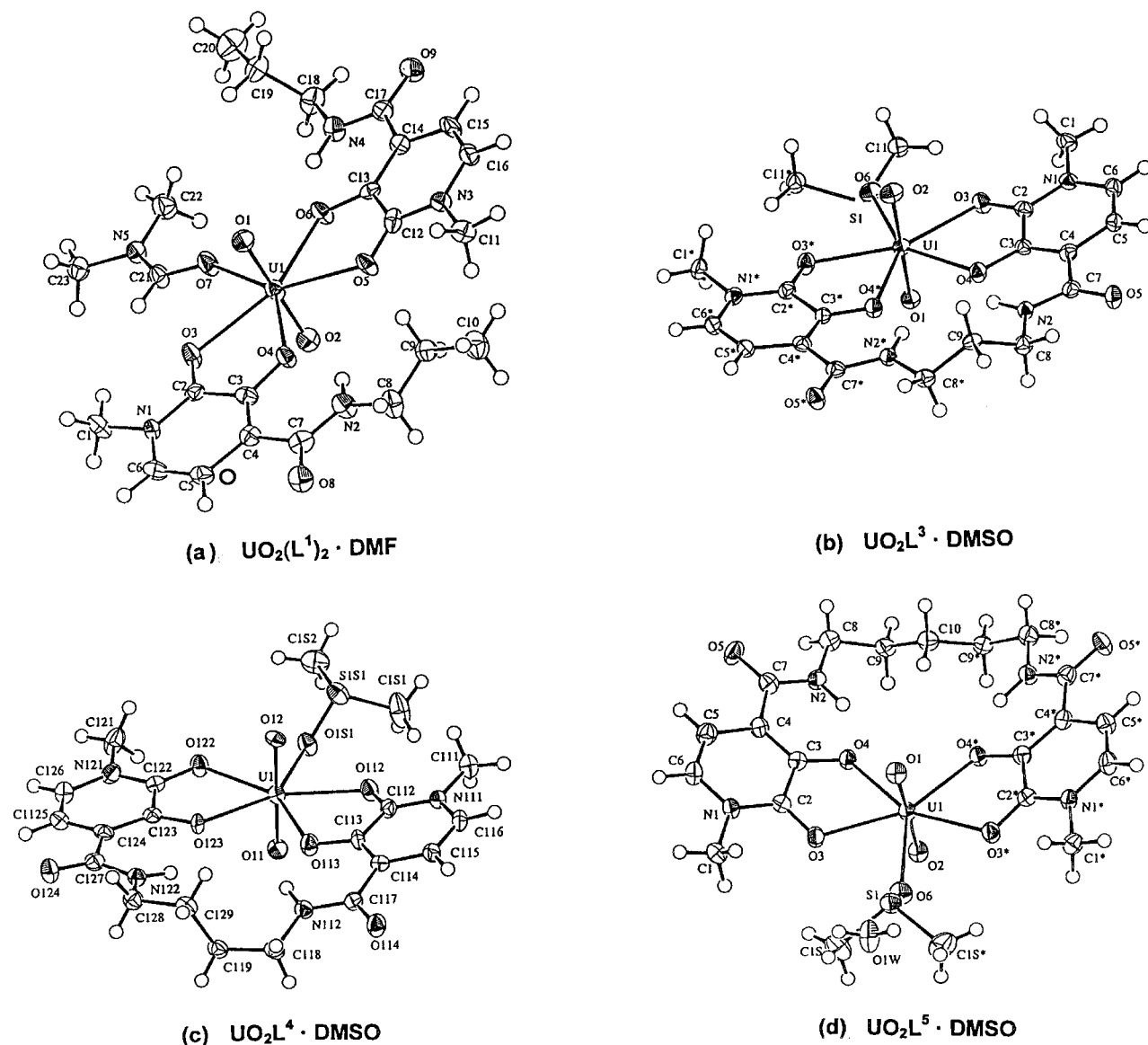
Figure 1. Crystal structures of (a) [UO$_2$(L^1)$_2$·DMF], (b) [UO$_2$L^3·DMF], (c) [UO$_2$L^4·DMF], and (d) [UO$_2$L^5·DMF] (ORTEP drawing). Thermal ellipsoids are drawn at the 50% probability level. See Chart 2 for the ligand structures.

A tetradentate Me-3,2-HOPO should be a good chelator for the uranyl ion because (1) a tetradentate chelator is far more effective than a bidentate monomer at low concentration in vivo (10^{-6} M or less);[4] (2) a tetradentate ligand should have less affinity than a hexadentate one for the biologically important metal ion Fe(III) thereby gaining selectivity; and (3) a tetradentate chelator with proper geometry can bind uranyl ion equatorially and leave the fifth equatorial coordination site for another small oxygen donating ligand such as water. Based on these considerations, a series of tetradentate Me-3,2-HOPO ligands, differing only in the length of the linear linker, was synthesized (Chart 2). To investigate the influence of rigidity of the ligands on the stability of the resulting uranyl complexes the more rigid ligands 2LI-Me-3,2-HOPO (H$_2$L^2) and ^{1R,2R}Cy-Me-3,2-HOPO (H$_2$L^8) were also prepared (Chart 2).

Structure of Uranyl-Bidentate Me-3,2-HOPO Complex [UO$_2$(L^1)$_2$·DMF]. Figure 1a shows the structure of [UO$_2$(L^1)$_2$·DMF], and selected bond lengths and angles are given in Table 2. The uranyl ion is equatorially pentacoordinate with four HOPO oxygen atoms and one solvent (DMF) oxygen atom. The uranium atom lies in the middle of the mean plane defined by the four HOPO oxygens and one DMF oxygen (mean deviation

Table 2. Selected Bond Lengths (Å) and Angles (deg) for UO$_2$(L^1)$_2$·DMF

Bond Lengths			
U$-$O(1)	1.787(5)	U$-$O(2)	1.779(6)
U$-$O(3)	2.457(5)	U$-$O(4)	2.329(5)
U$-$O(5)	2.407(5)	U$-$O(6)	2.374(5)
U$-$O(7)	2.371(5)		

Bond Angles			
O(1)$-$U$-$O(2)	179.37(14)	O(1)$-$U$-$O(3)	90.3(2)
O(1)$-$U$-$O(4)	89.1(2)	O(1)$-$U$-$O(5)	91.6(2)
O(1)$-$U$-$O(6)	89.8(2)	O(1)$-$U$-$O(7)	89.9(2)
O(3)$-$U$-$O(4)	66.4(2)	O(5)$-$U$-$O(6)	66.6(2)
O(4)$-$U$-$O(5)	76.8(2)	O(3)$-$U$-$O(7)	74.2(2)
O(6)$-$U$-$O(7)	76.1(2)	O(3)$-$U$-$O(5)	143.1(2)
O(3)$-$U$-$O(6)	150.3(2)	O(4)$-$U$-$O(5)	143.4(2)
O(4)$-$U$-$O(7)	140.5(2)	O(7)$-$U$-$O(5)	142.7(2)

from plane is 0.025 Å): it also lies in the middle of the mean plane defined by two uranyl oxygens and the DMF oxygen (mean deviation from plane is 0.000 Å). The two least-squares planes are essentially perpendicular, forming a dihedral angle of 89.52 °. The bond length of uranyl to the solvent (DMF) oxygen donor U$-$O7 is 2.371(5) Å, as compared with that of the phenolic oxygens of [UO$_2$(L^1)$_2$·DMF] (2.329(5) and 2.374-

Table 3. Selected Bond Lengths (Å) and Angles (deg) for UO$_2$L^3·DMSO

Bond Lengths			
U(1)−O(1)	1.783(4)	U(1)−O(2)	1.783(4)
U(1)−O(3)	2.410(3)	U(1)−O(4)	2.350(3)
U(1)−O(6)	2.357(4)		

Bond Angles			
O(1)−U(1)−O(2)	178.5(2)	O(3)−U(1)−O(4)	66.88(9)
O(4)−U(1)−O(4*)	72.33(13)	O(6)−U(1)−O(3)	76.94(7)
O(1)−U(1)−O(3)	90.52(8)	O(2)−U(1)−O(3)	89.14(8)
O(1)−U(1)−O(4)	91.62(12)	O(2)−U(1)−O(4)	89.59(13)
O(1)−U(1)−O(6)	89.1(2)	O(2)−U(1)−O(6)	89.4(2)

(5) Å, respectively), indicating strong coordination by the DMF oxygen donor.

Both of the 3,2-HOPO rings and their attached oxygen atoms are coplanar to within 0.01 Å. The atoms of both 3,2-HOPO amide groups (C4, C7, N2, O8 and C14, C17, N4, O9) are coplanar (mean deviation from planarity of 0.004 and 0.002 Å, respectively). The HOPO ring planes and their attached amide planes are slightly twisted, forming dihedral angles of 2.99 and 1.82°, respectively. The average distance between the amide nitrogens and their adjacent phenolic oxygens, 2.721(8) Å, shows a strong hydrogen bond between the amide protons and the oxygen donor atoms.

Structure of Uranyl−Tetradentate Me-3,2-HOPO Complexes. The structures of the tetradentate Me-3,2-HOPO uranyl complexes are similar to that of the bidentate Me-3,2-HOPO uranyl complex. Four of the equatorially ligating atoms are from two HOPO units of the ligand and the remaining coordination site is occupied by the solvent (DMSO) oxygen atom. Similar to the bidentate complex, the average U−O(solvent) bond length (2.358(5) Å) is close to that of U−O$_{phenol}$ (2.362(4) Å), much shorter than that of U−O$_{oxo}$(HOPO) (2.426(4) Å) in the tetradentate complexes. Remarkably, this shows stronger coordination by the coordinated solvent (DMSO) oxygen donor than by the HOPO oxo donor. Unique aspects of each of the complexes will now be presented.

UO$_2$-3LI-Me-3,2-HOPO Complex [UO$_2$L^3·DMSO]. There is only half a molecule in each asymmetric unit (*Pnma*; *Z* = 4). The molecular structure of [UO$_2$L^3·DMSO] is illustrated in Figure 1b; selected intramolecular bond lengths and angles are given in Table 3. The uranyl ion is equatorially pentacoordinate and planar, from four HOPO oxygen atoms and one solvent (DMSO) oxygen atom (O3, O4, O5, O3*, O4*) (mean deviation from planarity is 0.020 Å). The U(VI) atom is slightly (0.024 Å) above the least-squares plane defined by the four HOPO oxygen atoms(O3, O4, O3*, O4*) and the DMSO oxygen donor O5; the uranium (VI) atom with its oxo atoms (O1, O2) and the DMSO oxygen atom (O5) lie in the crystallographic mirror plane.

The 3,2-HOPO ring and attached oxygen atoms (N1, C2, C3, C4, C5, C6, O3, O4) are coplanar to within 0.008 Å. The atoms of the amide group (C4, C7, N2, O6) are also coplanar to within 0.008 Å. These two planes are slightly twisted, forming a dihedral angle of 9.38°. The distance of the amide nitrogen N2 to its adjacent phenolic oxygen O4 is 2.700 (4) Å, shorter than that in [UO$_2$(L^1)$_2$·DMF], showing a strong hydrogen bond between the amide proton and the oxygen donor atom.

UO$_2$-4LI-Me-3,2-HOPO Complex [UO$_2$L^4·DMSO]·DMSO· H$_2$O·0.5C$_6$H$_{12}$. The structure conforms to *P2$_1$/n* (*Z* = 8) with two discrete [UO$_2$L^4·DMSO] complexes, two noncoordinated DMSO, two water molecules and one cyclohexane molecule (disordered) in each asymmetric unit. The molecular structure of [UO$_2$L^4·DMSO] is illustrated in Figure 1c, all noncoordinated

Table 4. Selected Bond Lengths (Å) and Angles (deg) for [UO$_2$L^4·DMSO]·DMSO·H$_2$O·0.5C$_6$H$_{12}$

complex 1		complex 2	
Bond Lengths			
U(1)−O(11)	1.779(5)	U(2)−O(21)	1.769(5)
U(1)−O(12)	1.760(4)	U(2)−O(22)	1.774(5)
U(1)−O(112)	2.434(4)	U(2)−O(212)	2.433(5)
U(1)−O(113)	2.355(4)	U(2)−O(213)	2.364(4)
U(1)−O(122)	2.421(4)	U (2)−O(222)	2.432(5)
U(1)−O(123)	2.360(4)	U(2)−O(223)	2.351(4)
U(1)−O(1S1)	2.369(5)	U(2)−O(2S1)	2.366(5)
Bond Angles			
O(11)−U(1)−O(12)	178.6(2)	O(21)−U(2)−O(22)	178.3(2)
O(112)−U(1)−O(113)	66.6(2)	O(212)−U(2)−O(213)	66.1(1)
O(113)−U(1)−O(123)	79.8(2)	O(213)−U(2)−O(223)	80.1(2)
O(122)−U(1)−O(123)	66.2(2)	O(223)−U(2)−O(222)	66.6(2)
O(122)−U(1)−O(1S1)	75.0(2)	O(222)−U(2)−O(2 S1)	73.1(2)
O(1S1)−U(1)−O(112)	72.7(2)	O(2S1)−U(2)−O(212)	74.3(2)
O(11)−U(1)−O(112)	85.9(2)	O(21)−U(2)−O(212)	88.4(2)
O(12)−U(1)−O(112)	94.2(2)	O(22)−U(2)−O(212)	90.5(2)
O(11)−U(1)−O(1S1)	91.3(2)	O(21)−U(2)−O(2S1)	88.1(2)
O(12)−U(1)−O(1S1)	87.4(2)	O(22)−U(2)−O(2S1)	90.3(2)

Table 5. Selected Bond Lengths (Å) and Angles (deg) for UO$_2$L^5·DMSO

Bond Lengths			
U(1)−O(1)	1.775(4)	U(1)−O(2)	1.776(4)
U(1)−O(3)	2.442(3)	U(1)−O(4)	2.379(3)
U(1)−O(6)	2.349(4)		

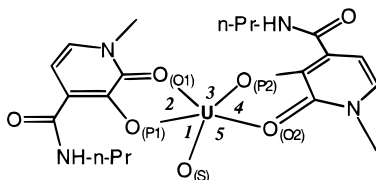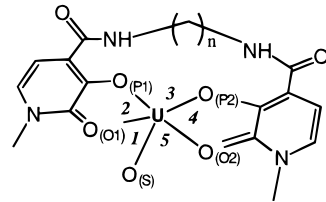| Bond angles			
O(1)−U(1)−O(2)	178.8(2)	O(3)−U(1)−O(4)	65.96(9)
O(4)−U(1)−O(4*)	90.26(14)	O(6)−U(1)−O(3)	69.87(7)
O(1)−U(1)−O(3)	84.29(8)	O(2)−U(1)−O(3)	95.29(8)
O(1)−U(1)−O(4)	91.23(12)	O(2)−U(1)−O(4)	89.59(12)
O(1)−U(1)−O(6)	94.9(2)	O(2)−U(1)−O(6)	83.9(2)

solvents were omitted for clearity. Since the two crystallographically independent molecules are nearly identical, only one is shown in the Figure. The selected intramolecular bond lengths and angles are given in Table 4.

UO$_2$-5LI-Me-3,2-HOPO Complex [UO$_2$ L^5·DMSO]·DMSO. This structure also conforms to *Pnma* (*Z* = 4); each asymmetric unit contains half a complex and half of a noncoordinated DMSO molecules. The molecular structure of [UO$_2$L^5·DMSO] is illustrated in Figure 1d, and selected intramolecular bond lengths and angles are given in Table 5. The distance between the amide nitrogen and its adjacent phenolic oxygen atoms, 2.765(4) Å, is the longest compared with other uranyl complex structures described in this paper, indicating relatively weaker hydrogen bonding.

Comparison of the Structures of Uranyl−Tetradentate Me-3,2-HOPOs. All of the uranyl complex structures are similar (Figure 1). They are comprised of one uranyl, one tetradentate 3,2-HOPO ligand and one coordinated solvent molecule (DMSO). Each U(VI) is coordinated by seven oxygen atoms in a slightly distorted pentagonal bipyramidal geometry. In all of these uranyl complexes, the 3,2-HOPO rings and their attached oxygen atoms are coplanar (within 0.008−0.02 Å) as are the atoms of the amides (within 0.01 Å). The amide planes and their attached 3,2-HOPO ring planes are slightly twisted. There is strong hydrogen bonding between the amide nitrogen protons and their adjacent phenolic oxygen atoms.

Complex Conformation and the Linear Linker Length of the Ligand. Although the structures of these uranyl complexes are similar, some consistent differences are apparent. The HOPO to uranium bite angle (defined by O$_{oxo}$(HOPO)−U−O$_{phenol}$) is essentially constant (from 66.2 to 66.9°, Table 6). However,

Table 6. Comparison of Equatorial Bond Angles (deg) of Uranyl Me-3,2-HOPO Complexes[a,b]

	UO$_2$(L^1)$_2$ (DMF)	UO$_2$L^3 (DMSO) (n = 3)	UO$_2$L^4 (DMSO) (n = 4)	UO$_2$L^5 (DMSO) (n = 5)
angle 1	74.2(2)	76.94(7)	72.7(2)	69.87(7)
angle 2	66.4(2)	66.88(9)	66.6(2)	65.96(7)
angle 3	76.8(2)	72.33(13)	79.8(2)	90.26(14)
angle 4	66.7(2)	66.88(9)	66.2(2)	65.96(9)
angle 5	76.1(2)	76.94(7)	75.0(2)	69.87(7)

[a] Uranyl oxo atoms were omitted for clarity. [b] O$_{(O1)}$ and O$_{(O2)}$ are the abbreviations of HOPO oxo donors O$_{(Oxo1)}$ and O$_{(Oxo2)}$, respectively; O$_{(P1)}$ and O$_{(P2)}$ are the abbreviations of HOPO phenol oxygen donors O$_{(Phenol1)}$ and O$_{(Phenol2)}$, respectively. O$_{(S)}$ is the abbreviation of O$_{(Solvent)}$.
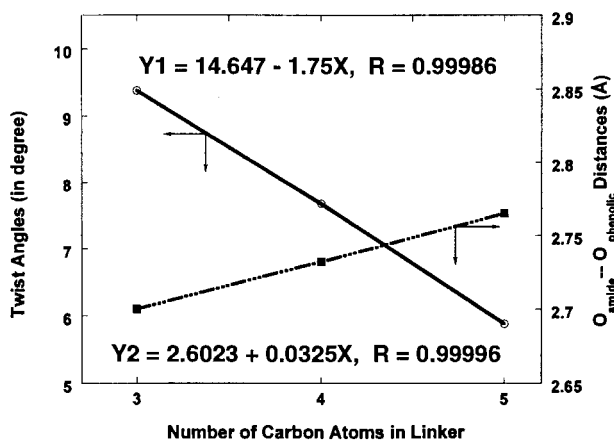
Figure 2. Amide twist angles and amide hydrogen bond lengths in uranyl−tetradentate Me-3,2-HOPOs (O, amide twist angle; ■, amide hydrogen bond length).

the change of linker length has a great influence on the equatorial plane configuration. As the length of linker increases, the angle formed between the uranium and two phenolic oxygen donors also becomes greater, from 72.3° in [UO$_2$L^3·DMSO] to 90.26° in [UO$_2$L^5·DMSO]. This angle in the unconstrained bidentate complex [UO$_2$(L^1)$_2$·DMF] is 76.8° (compared with 72° for the ideal pentagon). In [UO$_2$L^4·DMSO] the angle is 79.8°, indicating that there is little strain in this complex caused by the linker. The linker length of [UO$_2$L^3] is too short, while that in [UO$_2$L^5] is too long, both causing strain in the molecule and forcing the bite angle O$_{(p1)}$−U−O$_{(p2)}$ to be smaller or greater than the "unconstrained" value in the bidentate complex [UO$_2$(L^1)$_2$· DMF] (Table 6). As the linker chain length increases and the angle of the uranium with two phenolic oxygen atoms also increases, the angles of uranium with the solvent oxygen and its adjacent oxygen (pyridinone oxo) correspondingly decrease.

As a result of the strain imposed by the linker, the strength of the amide hydrogen bonds in these uranyl complexes also change in the following sequence: UO$_2$L^3 (2.700(4)) > UO$_2$-(L^1)$_2$ (2.721(8)) > UO$_2$L^4 (2.732(4)) > UO$_2$L^5 (2.765(4)). The strength of amide hydrogen bonding is also linearly correlated with the linker length (Figure 2). That four carbon atoms may be considered the optimal length is consistent with the high efficacy of H$_2$L^4 for in vivo uranyl chelation.[28,29]

Due to π conjugation, the 3,2-HOPO ring and its attached amide group are expected to be coplanar. However, the amide planes in the uranyl−tetradentate HOPO complexes are slightly twisted with respect to the HOPO ring planes. This change in

twist angle is also linearly correlated with the length of the chain in the linker of these complexes (Figure 2): 9.38° (in [UO$_2$L^3· DMSO]) > 7.68° (in [UO$_2$L^4·DMSO]) > 5.88° (in [UO$_2$L^5· DMSO]).

Figure 3 (side view) shows the dihedral angle between two pyridinone ring planes in [UO$_2$(L^1)$_2$·DMF], [UO$_2$L^3·DMSO], [UO$_2$L^4·DMSO], and [UO$_2$L^5·DMSO]. This angle is 170.32° (average value) in [UO$_2$ L^4·DMSO], close to that in [UO$_2$(L^1)$_2$· DMF] (171.65°), while these angles in [UO$_2$L^5·DMSO], and [UO$_2$L^3·DMSO] are 166.6° and 141.14°, respectively, giving these molecules a ruffled shape. The magnitude of this dihedral angle correlates with the strain in the linear linker. The reorganization energies for the bridge portion of the ligand, defined as the difference between the lowest energy (MM2 calculation) of the ligand coordinated to the metal (as found in the crystal structure) and the lowest energy free ligand conformation increase in the sequence of [UO$_2$L^4·DMSO], [[UO$_2$L^3· DMSO], [UO$_2$L^5·DMSO].[35] Thus the uranyl-bidentate complex [UO$_2$(L^1)$_2$·DMF] (which has no linker) should have no strain, while compound [UO$_2$L^5·DMSO] (which has the longest linear linker) is the most strained.

In solution, these achiral uranyl−tetradentate Me-3,2-HOPO complexes are less rigid due to their flexible linear linker, and they undergo more thermal averaging of structure[36] than possible in the solid state. However this difference should not be very large in this family of compounds, since the uranyl coordination centers in these complexes are similar, and the motions of the linear linkers of these complexes are limited by the equatorial coordination geometry. It was observed that the amide chemical shifts correlate with the number of carbon atoms in the linear linkers (Figure 4). The amide proton chemical shift for UO$_2$L^2 complex, which has the shortest linear linker, is 10.99 ppm, and is the farthest downfield in this series of complexes. Since the downfield chemical shifts of amide protons are generally interpreted in terms of strong hydrogen bonding,[37] a monotonic relationship between the chemical shift of the amide proton and the length of the linear linker can be expected if these complexes in solution preserve the structures found in the solid state. Regression analysis of the experimental values for δ vs n (number of carbon atoms in linear linker), gave a quadratic fit of $\delta = 13.70 - 1.682n + 0.1659n^2$ with a correlation coefficient of 0.9998.

(35) *CAChe, version 3.9*; CAChe Scientific: 1996.
(36) Hoelger, C. G.; Agular-Parrila, F.; Elguero, J.; Weintraub, O.; Vega, S.; Limbach, H. H. *J. Magn. Reson. A* **1996**, *120*, 46−55.
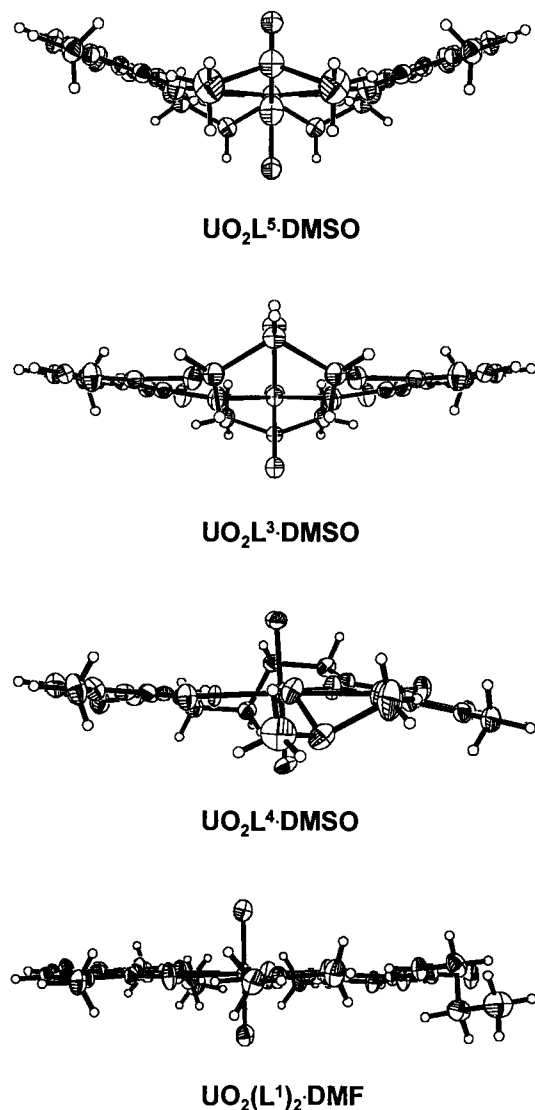(37) Buckingham, A. D. *Can. J. Chem.* **1960**, *38*, 300−307.

UO₂L⁵·DMSO

UO₂L³·DMSO

UO₂L⁴·DMSO

UO₂(L¹)₂·DMF

Figure 3. ORTEP diagrams (side views) and structural formulae of [UO₂(L¹)₂·DMF], [UO₂L³·DMSO], [UO₂L⁴·DMSO], and [UO₂L⁵·DMSO]. These comparisons show the differences in dihedral angle between two pyridinone rings of each molecule which result from the strain induced by the linker unit.

Conclusion

In summary, a rational design of uranyl sequestering agents based on 3-hydroxy-2(1*H*)-pyridinone has resulted in the first effective agents for mammalian uranyl decorporation. Crystals were difficult to obtain from aqueous solution but could be obtained by substituting dimethyl sulfoxide or dimethylformamide for water. The tetradentate ligand binds uranyl ion equatorially and a solvent molecule fills the fifth equatorial coordination site; in vivo, the fifth equatorial coordination site
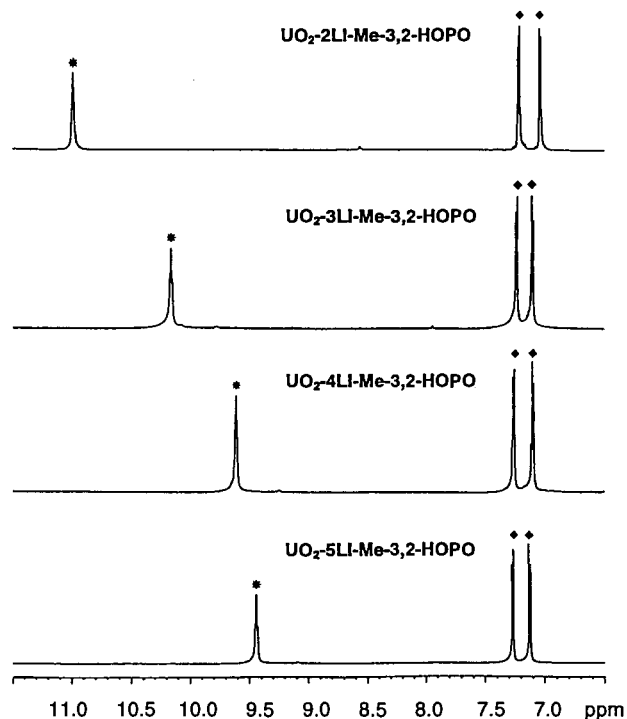

Figure 4. ^{1}H NMR chemical shifts in uranyl complexes with tetradentate Me-3,2-HOPO ligands (∗, amide proton; ◆, HOPO ring proton). Note the amide shift with linker length.

should be filled by a water molecule. The uranium and the five equatorial oxygen atoms are coplanar and the pyridinone ring atoms show a mean deviation of ca. 0.1 Å from their least-squares plane. The linker length affects the conformation of the complexes. The dihedral angles between two pyridinone ring planes also differ as the linker length changes, giving these molecules ruffled shape. The physical parameters (such as NMR chemical shifts) of the tetradentate Me-3,2-HOPO uranyl complexes correlate well with the length of the linker unit.

Supporting Information Available: X-ray structural data for [UO₂-(L²)₂·DMF], [UO₂L³·DMSO], [UO₂L⁴·DMSO]·DMSO·H₂O·0.5 C₆H₁₂, and [UO₂L⁵·DMSO]·DMSO including a summary of crystallographic parameters, atomic coordinates, bond distances and angles, and anisotropic thermal parameters (26 pages). Ordering instructions are given on any current masthead page.

IC980993Q